

---

## Modelling the Ionospheric and Plasmaspheric Plasma [and Discussion]

R. J. Moffett, G. J. Bailey, S. Quegan, Y. Rippeth, A. M. Samson and R. Sellek

*Phil. Trans. R. Soc. Lond. A* 1989 **328**, 255-270

doi: 10.1098/rsta.1989.0035

---

### Email alerting service

Receive free email alerts when new articles cite this article - sign up in the box at the top right-hand corner of the article or click [here](#)

---

To subscribe to *Phil. Trans. R. Soc. Lond. A* go to: <http://rsta.royalsocietypublishing.org/subscriptions>

---

## Modelling the ionospheric and plasmaspheric plasma

BY R. J. MOFFETT, G. J. BAILEY, S. QUEGAN, Y. RIPPETH, A. M. SAMSON  
AND R. SELLEK

*Department of Applied and Computational Mathematics, University of Sheffield,  
Sheffield S10 2TN, U.K.*

Under magnetically quiet conditions, the outer plasmasphere is the equatorward boundary of the region in which high-latitude processes, such as convection, significantly affect the ionosphere. The low-latitude side of the ionospheric mid-latitude trough is located in the plasmasphere. The behaviour of the nightside trough is influenced by field-aligned flows of plasma, as well as by convection drifts, thermospheric winds and particle precipitation. The modelling of field-aligned flow of thermal plasma at high latitudes (the polar wind) still presents problems. The composition of the background neutral atmosphere plays a role in causing the occasional dominance of  $\text{He}^+$  in the topside ionosphere. Penetration of magnetospheric electric fields into the outer plasmasphere can influence the rate of refilling of the upper reaches of the flux tubes.

### 1. INTRODUCTION

The meaning of the word ‘ionosphere’ is generally well known. The ionosphere is that region of the atmosphere that contains significant quantities of charged particles and it plays a significant role in the propagation of radio waves. Layers in the ionosphere have been given labels such as D, E and F. The topside ionosphere, that part of the ionosphere lying above the height of the peak of plasma concentration in the F-layer, merges into a region that may be called the ‘protonosphere’; the F-layer ions are mostly  $\text{O}^+$  whereas those of the protonosphere, as the name indicates, are largely  $\text{H}^+$ . In recent years the term ‘plasmasphere’ has been introduced. This has followed the use of the term ‘plasmopause’ to describe the often observed sharp gradient in the electron concentration at several Earth radii† in the equatorial plane. Thus in this terminology the plasmasphere contains all the plasma that is to be found equatorward and earthward of the plasmopause, and it includes the ionosphere of the equatorial and mid-latitude regions. The plasmaspheric plasma lies on closed magnetic flux tubes and essentially corotates with the Earth. However, the ionosphere extends into the high-latitude region (including the polar cap), beyond the projection of the plasmopause to F-layer heights. The term ‘plasmasphere’ is often used to describe the plasma above the ionosphere, i.e. that plasma that contains mostly light ions,  $\text{H}^+$  and  $\text{He}^+$ . Loose usage of ‘plasmasphere’ rarely causes confusion, in contrast to the use of ‘plasmopause’ or ‘trough’ when referring to phenomena in the equatorial plane or in the ionosphere (see below).

In the context of a discussion of high-latitude and magnetospheric processes, modelling of the plasmaspheric plasma is relevant from two aspects. The outer plasmasphere, adjacent to the plasmopause, forms the equatorward boundary of the high-latitude plasma régime. For example, the mid-latitude trough in the F-layer electron concentration, often associated with

†  $R_E = 6.37 \times 10^6$  m.

the plasmapause, may lie within the plasmasphere. Secondly, models of the high-latitude ionosphere had their genesis in models that were developed for studies of the plasmasphere. Both the mathematical structure of the high-latitude models and our understanding of the behaviour of the high-latitude ionosphere depend critically on the prior development of the theory of the plasmaspheric plasma.

In this paper, the physical processes relevant to the plasmasphere are listed and the equations that represent them are examined, with emphasis given to the plasma dynamics. The contributions that modelling can bring to topics such as the mid-latitude trough, magnetic field-aligned plasma flows, the polar wind and the occurrence of  $\text{He}^+$  ions at high latitudes are considered. Finally, some results are presented on convective  $\mathbf{E} \times \mathbf{B}$  drift effects in the mid-latitude plasmasphere.

## 2. PLASMASPHERIC PROCESSES AND INFLUENCE OF PLASMA DRIFTS

The thermal (less than about 1 eV energy) ionization of the plasmasphere is mainly produced by the action of solar extreme ultraviolet radiation on the neutral gases of the thermosphere. A further contribution arises at high latitudes from the ionizing effects of energetic particles precipitated from the magnetosphere. Chemical interactions of the primary ions with neutral gases produce other ions, which in turn may recombine with electrons. For example, practically all of the thermal proton population is produced by the accidentally resonant charge-exchange reaction of  $\text{O}^+$  ions with neutral atomic hydrogen and the significant presence of  $\text{NO}^+$  in the E- and F-regions is due to the reaction of  $\text{O}^+$  with neutral molecular nitrogen. The rates of these reactions may depend on the temperatures of the interacting species and on the states of excitation of the species (for example, the vibrational state of  $\text{N}_2$ ). The composition of the thermosphere thus plays a large part in determining not only the ion species produced by photoionization (such as  $\text{O}^+$ ,  $\text{He}^+$ ,  $\text{N}_2^+$ ,  $\text{O}_2^+$ ), but also those produced by chemical means (such as  $\text{H}^+$ ,  $\text{NO}^+$ ).

Transport of the plasma occurs by processes described as ‘diffusion’ and ‘drift’. Diffusion relative to the neutral air takes place along geomagnetic field lines and is driven by gravity, pressure gradients, thermal diffusion due to temperature gradients and space-charge electric fields due to slight separation of the electrons and positive ions. The diffusion is modified by ion–ion drag between the different ion species and by neutral air winds that blow in the thermosphere. The temperatures appearing in the diffusion equation depend on the heat balance of the plasma. The electrons are heated by fast photoelectrons and by heat conducted from the magnetosphere. Interspecies heat transfer (electron–ion, ion–ion, ion–neutral) and thermal conduction are also major processes.

Drift of the plasma is caused by an electric field,  $\mathbf{E}$ , imposed perpendicular to the geomagnetic field,  $\mathbf{B}$ . The drift velocity is given by  $\mathbf{E} \times \mathbf{B}/B^2$ . It is a fortunate circumstance that first attempts at numerical modelling of the F-layer plasma in equilibrium were applied in *mid-latitude* studies. For mid-latitudes,  $\mathbf{E} \times \mathbf{B}$  drift could be treated simply. Reasonable results can be produced in a vertical column of plasma by considering only the vertical component of the drift; this component can be treated in the same way as the effective vertical component of the thermospheric neutral air wind. This situation at mid-latitudes is in sharp contrast to those at equatorial latitudes and high latitudes. The equatorial or Appleton anomaly in plasma concentration is caused by upward  $\mathbf{E} \times \mathbf{B}$  drift driven by the E-layer dynamo. At high latitudes,

convective  $\mathbf{E} \times \mathbf{B}$  drift driven by the solar wind via the magnetosphere is a *sine qua non* for effective modelling. In §5 we point to the increasing interest in  $\mathbf{E} \times \mathbf{B}$  drift effects at mid-latitudes.

It is intriguing that at high latitudes, where horizontal transport of plasma is so important, the vertical component of the drift must not be neglected. Indeed, the effect of the vertical component of strong convection may mask other effects of strong convection such as increased recombination rates.

### 3. TRANSPORT EQUATIONS FOR THE PLASMA

For ion species  $i$ , the continuity equation that describes the dependence of ion concentration,  $N_i$ , on the spatial coordinates and on time  $t$  takes the form

$$\partial N_i / \partial t = P_i - L_i - \nabla \cdot (N_i \mathbf{v}_i), \quad (1)$$

where  $P_i$  and  $L_i$  are the production and loss terms (per unit volume per unit time), respectively, and  $\mathbf{v}_i$  is the bulk velocity. If  $\mathbf{v}_i$  is resolved into two components

$$\mathbf{v}_i = \mathbf{v}_i^\perp + \mathbf{v}_i^\parallel, \quad (2)$$

where  $\mathbf{v}_i^\perp$  is perpendicular to the magnetic field,  $\mathbf{B}$ , and  $\mathbf{v}_i^\parallel$  is parallel to the magnetic field, it is found that to a very good approximation in the F-layer and topside ionosphere the perpendicular component is given by (Kendall & Pickering 1967; Moffett 1979)

$$\mathbf{v}_i^\perp = (\mathbf{E}^\perp \times \mathbf{B}) / B^2, \quad (3)$$

where  $\mathbf{E}^\perp$  is the (externally imposed) electric field, perpendicular to  $\mathbf{B}$ . By using this resolution of  $\mathbf{v}_i$ , equation (1) can then be written

$$dN_i/dt = P_i - L_i - \nabla \cdot (N_i \mathbf{v}_i^\parallel) - N_i \nabla \cdot \mathbf{v}_i^\perp, \quad (4)$$

where

$$dN_i/dt = \partial N_i / \partial t + (\mathbf{v}_i^\perp \cdot \nabla) N_i \quad (5)$$

is the rate of change of concentration with respect to time following the motion of the plasma under the  $\mathbf{E} \times \mathbf{B}$  drift (or, put another way, following the motion of a magnetic flux tube).

As pointed out in the previous section, the field-aligned ion motion is driven by several competing forces. The importance of individual force terms depends on the ion species and on the altitude region. There are the additional complications that the momentum (or diffusion) equation for a particular species is coupled to the momentum equations for the other species and also to the moment equations of higher order, such as the heat flow equations. Schunk (1975) presented a general set of aeronomical transport equations that were based on the formulation of Grad (1949, 1958) and the collision terms of Burgers (1969). In Schunk's equations the different species were allowed to have separate bulk velocities and separate temperatures. The equations have been applied by St-Maurice & Schunk (1977) to the mid-latitude topside ionosphere. Collision-dominated conditions were assumed and Burgers's linear collision terms used; the equations, valid for small temperature differences and small bulk velocity differences between the species, were derived for a fully ionized three-component plasma (two ion species plus electrons). Conrad & Schunk (1979) extended the work of St-Maurice & Schunk (1977) to the condition of large temperature differences between the

interacting species by using Burgers's semilinear collision terms and also applied the equations of Schunk (1975) to a three-component partially ionized plasma (one ion species plus electrons plus neutral air), a case that is applicable to the F-region. The need to model situations in which  $\text{He}^+$  (as well as  $\text{O}^+$  and  $\text{H}^+$ ) may have significant abundances in the topside ionosphere led Quegan *et al.* (1981) to extend the work of St-Maurice & Schunk (1977) to the case of a fully ionized four-component plasma (three major ions species plus electrons), allowing for large temperature differences between the species as in the paper by Conrad & Schunk (1979).

No attempt has yet been made to include a neutral air constituent self-consistently in the Quegan *et al.* (1981) three-ion scheme to make the scheme applicable to a partially ionized plasma. Such an attempt might require the use of algebraic manipulation codes. The work by Conrad & Schunk (1979), however, showed that for an  $\text{O}^+$ -O mixture under F-region conditions thermal diffusion effects and the ordinary diffusion correction can be neglected. In the notation of Conrad & Schunk, in the thermal diffusion term in the  $\text{O}^+$  equation,  $\omega \nabla T_n + \omega^* \nabla T_i$ , the thermal diffusion coefficient  $\omega$  is significant, but the gradient  $\nabla T_n$  in the neutral air temperature is small; and although the ion temperature gradient  $\nabla T_i$  may be significant,  $\omega^*$  (the thermal mutual diffusion coefficient) is small. Thus a synthesis of the equations applicable to fully ionized plasma of the topside ionosphere and the equations applicable to partially ionized plasma of the F-region can be made as follows. On this occasion only a summary of the results is given; details of the derivations can be found in the papers referenced above.

For three ion species,  $i, j$  and  $k$ , and neutral species,  $n$ , it is found that, by eliminating the field-aligned electric field (obtained from the electron momentum equation) and the heat flow vectors for the ions and electrons, the field-aligned momentum equation for species  $i$  becomes

$$\begin{aligned} & (k/m_i) \{ T_i \nabla N_i / N_i + \nabla T_i + z_i T_e \nabla N_e / N_e \\ & \quad + (z_i - \gamma_i) \nabla T_e + (\beta_i \nabla T_i - \beta_{ij}^* \nabla T_j - \beta_{ik}^* \nabla T_k) \} - \mathbf{G} \\ & = -(\mathbf{v}_i - \mathbf{v}_j) [\nu_{ij}(1 - \Delta_{ij}) - R_{ijk} + R_{ikj}] \\ & \quad - (\mathbf{v}_i - \mathbf{v}_k) [\nu_{ik}(1 - \Delta_{ik}) - R_{ikj} + R_{ijk}] - (\mathbf{v}_i - \mathbf{v}_n) \nu_{in}, \end{aligned} \quad (6)$$

where for convenience the parallel signs have been omitted so that, for example,  $\mathbf{v}_i$  now represents  $\mathbf{v}_i^{\parallel}$ ,  $k$  is Boltzmann's constant,  $m_i$  is ion mass,  $\mathbf{G}$  is the acceleration due to gravity,  $z_i$  is ion charge,  $T_i$  is ion temperature,  $T_e$  is electron temperature,  $N_e = N_i + N_j + N_k$  is electron concentration,  $\nu_{st}$  is the binary collision frequency for momentum transfer between species  $s$  and species  $t$ ,  $\beta_i$  is the thermal (self-diffusion) coefficient for species  $i$ ,  $\beta_{ij}^*$  is the thermal (mutual) diffusion coefficient for species  $i$  corresponding to a gradient in the temperature of species  $j$  and  $\beta_{ik}^*$  is the thermal (mutual) diffusion coefficient for species  $i$  corresponding to a gradient in the temperature of species  $k$ . Expressions for these diffusion coefficients, the diffusion coefficient,  $\gamma_s$ , and the correction factors,  $\Delta_{st}$  and  $R_{stu}$ , are given by Quegan *et al.* (1981). For modelling calculations, it is usual to derive an explicit expression for  $\mathbf{v}_i$  to substitute in continuity equation (4). From (6), such an expression is

$$\begin{aligned} \mathbf{v}_i & = h_{ij} \mathbf{v}_j + h_{ik} \mathbf{v}_k + h_{in} \mathbf{v}_n \\ & \quad - \mathcal{D}_i \{ \nabla N_i / N_i + \nabla N_e / N_e - (m_i \mathbf{G}) / (k T_i) + z_i (T_e / T_i) \nabla N_e / N_e \\ & \quad \times (z_i - \gamma_i) \nabla T_e / T_i + (\beta_i \nabla T_i - \beta_{ij}^* \nabla T_j - \beta_{ik}^* \nabla T_k) / T_i \}, \end{aligned} \quad (7)$$



where, for ion species  $s$ ,  $t$  and  $u$ ,

$$h_{st} = (\nu_{st}(1 - A_{st}) - R_{stu} + R_{sut}) / (\nu_{st}(1 - A_{st}) + \nu_{su}(1 - A_{su}) + \nu_{sn}), \quad (8)$$

and, for ion species  $s$  and neutral species  $n$ ,

$$h_{sn} = \nu_{sn} / (\nu_{st}(1 - A_{st}) + \nu_{su}(1 - A_{su}) + \nu_{sn}). \quad (9)$$

The quantity

$$\mathcal{D}_s = kT_s / [m_s(\nu_{st}(1 - A_{st}) + \nu_{su}(1 - A_{su}) + \nu_{sn})] \quad (10)$$

may be termed the 'ordinary diffusion coefficient' for species  $s$ . It may be noted that  $h_{st} + h_{su} + h_{sn} = 1$ ; and that, although  $\mathcal{D}_s$  does not depend on the  $R$  terms, the  $h$  quantities do.

The accuracy of the various transport coefficients can be determined only in the limit of equal species temperatures (Conrad & Schunk 1979). For a fully ionized plasma the coefficients are accurate to within 20–30% and for a partially ionized plasma to within 5%.

From (7) the field-aligned flux,  $N_i \mathbf{v}_i$ , may be written as

$$N_i \mathbf{v}_i = -X_i \nabla N_i - Y_i N_i, \quad (11)$$

where

$$X_i = \mathcal{D}_i [1 + (T_e/T_i)(N_i/N_e)] \quad (12)$$

and

$$\begin{aligned} Y_i = & -(h_{ij} \mathbf{v}_j + h_{ik} \mathbf{v}_k + h_{in} \mathbf{v}_n) \\ & + \mathcal{D}_i \{ \nabla T_i / T_i - (m_i \mathbf{G}) / (kT_i) + z_i (T_e/T_i) \nabla (N_j + N_k) / N_e \\ & + (z_i - \gamma_i) \nabla T_e / T_i + (\beta_i \nabla T_i - \beta_{ij}^* \nabla T_j - \beta_{ik}^* \nabla T_k) / T_i \}. \end{aligned} \quad (13)$$

If  $X_i$  is written as

$$X_i = (k/m_i) \{ T_i + T_e (N_i/N_e) \} / (\nu_{ij}(1 - A_{ij}) + \nu_{ik}(1 - A_{ik}) + \nu_{in}), \quad (14)$$

it is more easily recognized to be a modified 'ambipolar' diffusion coefficient; with only  $O^+$  ions and neutrals present,  $X_i = k(T_i + T_e)/m_i \nu_{in}$ . Then the continuity equation (4) becomes the diffusion equation

$$dN_i/dt = A_i \partial^2 N_i / \partial s^2 + B_i \partial N_i / \partial s + C_i N_i + D_i, \quad (15)$$

where  $|\nabla^{\parallel}|$  has been replaced by  $\partial/\partial s$ ,  $\nabla \cdot (N_i \mathbf{v}_i^{\parallel})$  has been replaced by  $B \partial/\partial s (N_i v_i^{\parallel}/B)$ ,  $s$  being the arc length coordinate along the magnetic field, and where

$$A_i = X_i, \quad (16)$$

$$B_i = X_i B \partial B^{-1} / \partial s + \partial X_i / \partial s + Y_i, \quad (17)$$

$$C_i = Y_i B \partial B^{-1} / \partial s + \partial Y_i / \partial s - \nabla \cdot \mathbf{v}_i^{\perp}, \quad (18)$$

$$D_i = P_i - L_i. \quad (19)$$

It can be observed that both the coefficients  $X_i$  and  $Y_i$  (and thus  $A_i$ ,  $B_i$  and  $C_i$ ) contain terms involving  $N_i$ ,  $N_j$  and  $N_k$ , the dependent variables for which the solutions of (15) and corresponding equations are required. This linearization of the nonlinear system of transport equations is mentioned in the next section.

The ion temperatures and electron temperature appear in the diffusion equation (15). In recent modelling studies, the values of these temperatures have been obtained by solving the heat balance equations for the ions and electrons. It is not proposed to quote these equations

in this paper. Typical equations applicable to low latitudes and mid-latitudes may be found, for example, in the paper by Bailey *et al.* (1986).

Moffett (1988) has discussed the validity of the heat transfer terms currently used in heat balance equations. It was concluded that, until a recalculation is performed of the atomic oxygen fine structure collision strengths, it must be presumed that the currently available values are reliable. Thus the commonly used version of the electron fine structure cooling rate is reliable if the degree of non-equilibrium of the fine structure levels is known. Work by Ogawa (1982) on interpretation of atomic oxygen 1304Å triplet airglow observations and by Iwagami & Ogawa (1982) on atomic oxygen 63  $\mu\text{m}$  emission has shown that, in the lower thermosphere, local thermodynamic equilibrium of the fine structure levels at the ambient gas temperature is likely to hold. Moffett (1988) also pointed out that recent discussions of the validity of the widely used solar radiation fluxes and of the vibrational excitation rate of molecular nitrogen lend uncertainty to electron temperature calculations.

#### 4. NUMERICAL MODELLING CONSIDERATIONS

For closed magnetic field lines in the plasmasphere, the parabolic partial differential equation (15) is usually solved along a magnetic flux tube from a base level such as 120 km altitude to the equatorial plane or to the same level in the other hemisphere. A finite-difference scheme is used with the arc length,  $s$ , and time,  $t$ , as the independent variables. The nonlinearity inherent in (15) is treated by using values of the concentration and temperature variables that are available at the most recent time in the integration. Special care has to be exercised in this respect for calculations around sunrise and sunset when conditions usually change rapidly. On closed field lines the boundary conditions adopted at the base level are those applicable to photochemical equilibrium, i.e.  $P_1 = L_1$ . A small, artificial production may be required at night to avoid numerical instability. Results above a few spatial steps from the base level are not affected.

On open field lines at high latitudes, the upper boundary condition is usually a condition on the field-aligned ion velocities. Theoretical values for the velocities at high altitudes have not been derived (a deficiency in present models of the polar wind) and empirical estimates have to be used (Quegan *et al.* 1982; Allen *et al.* 1986). On the other hand, as indicated by results to be presented in this paper (§5), the precise values adopted for the ion velocities at a particular great height do not appear to affect significantly the average fluxes of  $\text{H}^+$  and  $\text{He}^+$  ions in the topside ionosphere.

Computational problems at high altitudes were experienced in modelling calculations when the denominator in expressions (8), (9) and (10), i.e.

$$\nu_{\text{st}}(1 - A_{\text{st}}) + \nu_{\text{su}}(1 - A_{\text{su}}) + \nu_{\text{sn}} \quad (20)$$

became small, leading to a very large diffusion coefficient in (15). With only one ion,  $\text{O}^+$ , expression (20) collapses to  $\nu_{\text{sn}}$ , which is proportional to  $n(\text{O})$ . Hanson & Moffett (1966) and Sterling *et al.* (1969), for example, found that the  $\text{O}^+ - \text{O}$  collision frequency had to be held at a uniform value at high altitudes in calculations relevant to low latitudes. It is not clear if this feature persists in the equatorial section of the global ionosphere model of Schunk & Sojka (1985). The inclusion of  $\text{H}^+$  as a second ion removed this difficulty (Moffett & Hanson 1973) for low latitudes. For mid-latitudes, however, where the equatorial crossing point altitude may

exceed 20 000 km the difficulty persisted unless small steps in the spatial coordinate were used. A numerical method to overcome this was described by Bailey *et al.* (1987). It can now be reported that because the latest models, from which results will be presented in §5 of this paper, include  $\text{He}^+$  (as well as  $\text{H}^+$ ) as a major ion, there is always sufficient abundance of another ion to cause (20) to have a significant magnitude. It is satisfying, indeed, that a more physically realistic model overcomes this particular computational problem.

The strong nonlinearity in the terms that express the electron heat loss to fine structure excitation of atomic oxygen and to vibrational excitation of molecular nitrogen demand great care in the numerical solution of the heat balance equations. Also, precise calculation of the heat input to the electron gas from photoelectron cooling is rendered difficult because of uncertainties in collision cross sections. Calibration of this heat input is hampered by the sparseness of mid-latitude, high-altitude ion and electron temperature observations. These modelling difficulties carry over to high-latitude calculations (Schunk 1987). Moreover, on the open field lines in the polar cap and on the closed field lines in the auroral zone, the heat flux from great altitudes is variable and uncertain. Schunk *et al.* (1986) made parametric studies of the effects of magnetospheric heat fluxes on the electron temperature of the F-region; the heat flux was found to control the temperature profile at altitudes above *ca.* 200 km and was particularly effective in the mid-latitude trough due to the low electron concentrations. Schunk *et al.* conclude that much work is needed to quantify the heat flux. It is more usual in high-latitude calculations to assume an empirical form for electron temperature and calculate the ion temperature.

## 5. MODEL RESULTS

### (a) Helium ion behaviour

The importance of thermospheric composition as the necessary background to modelling the plasma was mentioned in §2. Results from the coupling of the University College London (UCL) thermosphere model of the major neutral constituents and the Sheffield high-latitude ionosphere model show the importance of generating self-consistent thermospheric and ionospheric behaviour (Fuller-Rowell *et al.* 1987; Rees & Fuller-Rowell, this Symposium). The coupled model will in due course be extended to lower latitudes. In the meantime, it is customary to adopt an empirical model of the thermosphere, such as one of the mass spectrometer and incoherent scatter (MSIS) models, as input to the plasma models.

The role played by thermospheric composition will be exemplified by considering model results for  $\text{He}^+$ . This study was motivated by the availability of experimental data from observations on the satellite *Dynamics Explorer 2 (DE2)*. Observed data for the topside ionosphere are displayed in figure 1. The ion  $\text{He}^+$  is clearly dominant over both  $\text{O}^+$  and  $\text{H}^+$  in the region between 30 and 40° latitude at an altitude of *ca.* 900 km, with  $\text{He}^+$  the major light ion elsewhere. These particular data have been simulated by Heelis *et al.* (1989).

Model nighttime results for a dip latitude of 50° are shown in figure 2. It can be seen that a region of  $\text{He}^+$  dominance has appeared at around midnight and persists until dawn. These results for winter solstice show stronger  $\text{He}^+$  dominance than do results for equinox (not shown here), due to the winter bulge in neutral helium incorporated empirically into the MSIS models. In summer no  $\text{He}^+$  dominance is predicted. It can be observed also that at around 50° latitude the  $\text{He}^+$  feature appears later than the 22h00 LT feature of figure 1. The regions of  $\text{He}^+$



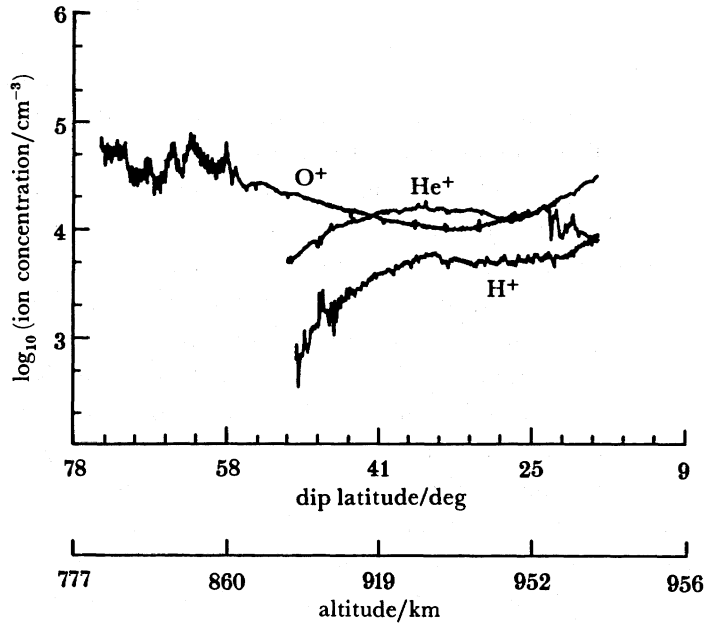


FIGURE 1. Ionospheric composition measurements made near 900 km altitude at 22h00 LT (4 October 1981) by the retarding potential analyser on board the *DE2* satellite (Heelis *et al.* 1989). These measurements were made near longitude  $152^\circ$  and show a latitude region where  $\text{He}^+$  is the dominant ion; at other latitudes  $\text{He}^+$  is the dominant light ion.

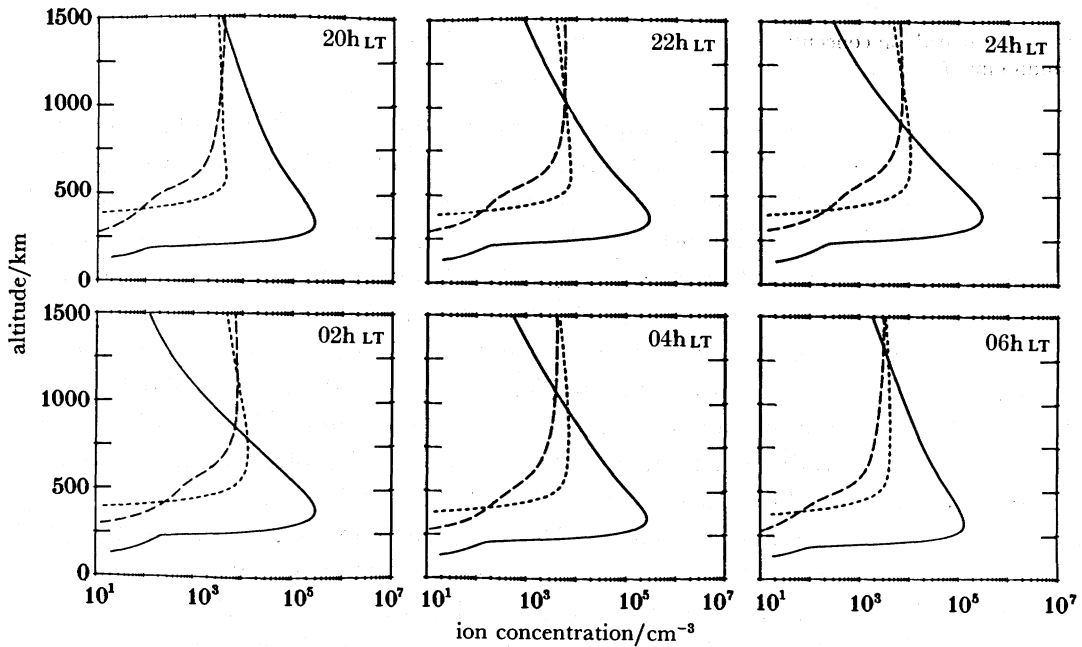


FIGURE 2. Nighttime altitude profiles of the modelled ion concentrations for winter solstice in the Northern Hemisphere at a dip latitude of  $50^\circ$ , with atmospheric conditions corresponding to  $F_{10.7} = 190$ : —,  $\text{O}^+$ ; ---,  $\text{H}^+$ ; ····,  $\text{He}^+$ .

dominance result from a combination of (i) the nighttime maintenance of  $\text{He}^+$  and (ii) the nighttime decrease in the  $\text{O}^+$  abundance associated with the diminished scale height.

In contrast to the solar maximum ( $F_{10.7} = 190$ ) results of figure 2, dominance of  $\text{He}^+$  is more likely at high latitudes at solar minimum. S. Quegan (this Symposium) has recalled calculations (Quegan *et al.* 1984) that show the conditions necessary for  $\text{He}^+$  dominance at high latitudes. A complementary plot is presented in figure 3. The diurnal variations of ion concentrations in the topside ionosphere lead to  $\text{He}^+$  dominance at 500 km altitude and above in the mid-latitude trough feature at winter solstice for  $F_{10.7} = 70$ . With greater solar activity ( $F_{10.7} = 150$ ) during winter, and during equinox and summer for all activity levels,  $\text{He}^+$  is a minor ion in the topside ionosphere.

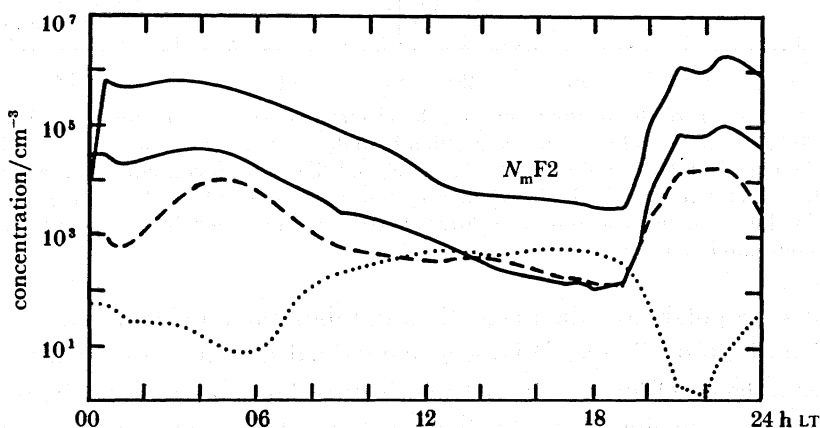


FIGURE 3. Modelled ion concentrations as a function of local time above the EISCAT facility at Tromsø: winter, solar minimum ( $F_{10.7} = 70$ ) conditions have been used. The upper curve shows the peak electron concentration in the F-layer; the other curves show the ion concentrations at 500 km altitude: —,  $\text{O}^+$ ; ---,  $\text{H}^+$ ; ····,  $\text{He}^+$ .

(b) *Nightside mid-latitude trough in electron concentration*

This feature of the mid-latitude F-layer and topside ionosphere has proved to be readily observable using satellite-borne and ground-based instruments. It is not to be confused with the 'light-ion trough' or 'main trough', although the mid-latitude ( $\text{O}^+$ ) trough may at times be magnetically collocated with these features and, indeed, may be synonymous with the main trough (Moffett & Quegan 1983; Muldrew 1983). The light-ion trough and main trough are essentially features in the  $\text{H}^+$  (and  $\text{He}^+$ ) distributions in the topside ionosphere and magnetosphere.

The mid-latitude trough as observed on the nightside is a subauroral phenomenon. This is illustrated in figure 4 by recent European incoherent scatter (EISCAT) radar observations (Collis & Häggström 1988). The high-latitude wall of the trough is produced by auroral ionization due to particle precipitation. In this time sector, the trough itself is due to the plasma being constrained to move slowly while shielded from the solar ionizing radiation. The quasi-stagnation region is caused by competition between westward convection and eastward corotation, an example of the very important consequences for the high-latitude ionosphere that arise from magnetospheric convection (S. Quegan, this Symposium).

The equatorward side of the trough merges into the outer region of the mid-latitude plasmasphere. Plasma in this region does not partake, in magnetically quiet times, in

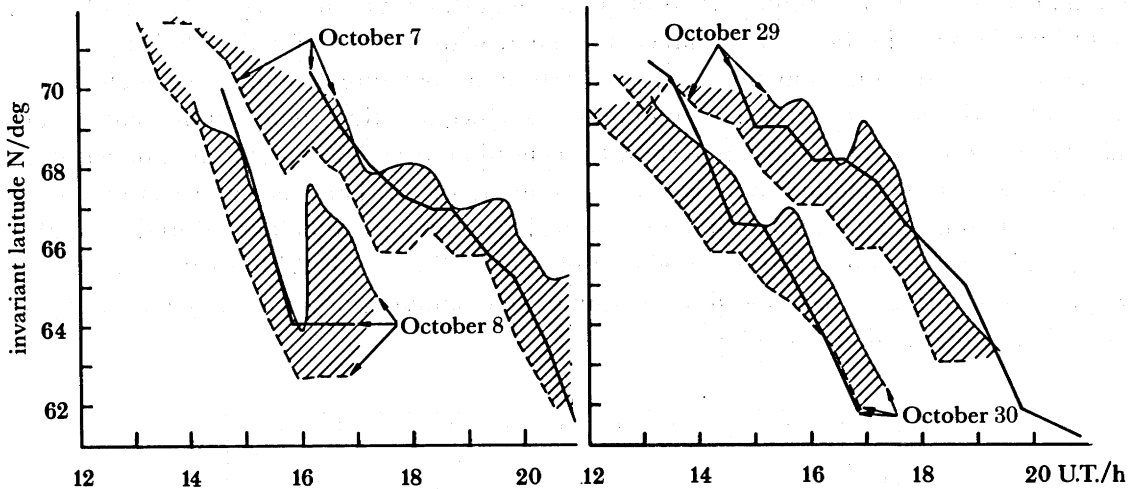


FIGURE 4. EISCAT observations of the relation between the electron concentration contour of  $9 \times 10^4 \text{ cm}^{-3}$  in the E-region at 120 km altitude (full line), the convection boundary separating flows with velocities greater than and less than  $300 \text{ m s}^{-1}$  at 275 km altitude (broken line) and the electron concentration minimum within the mid-latitude trough at 275 km altitude (heavy line) for four cases studied by Collis & Häggström (1988). The convection boundary and the E-region concentration contour are joined by hatched lines, which usually confine the trough minimum.

convection across the polar cap; the magnetic flux tubes remain closed and roughly dipolar. The nightside mid-latitude F-layer is largely maintained by equatorward neutral air winds raising the layer to levels of low recombination. Return flows of  $\text{H}^+$  from the protonosphere, however, also make a contribution to the maintenance. This is demonstrated in figures 5 and 6. The F-layer peak electron concentrations along the magnetic meridian through the EISCAT Tromsø location show the mid-latitude trough moving equatorward before midnight, with a return to higher latitudes approaching dawn (results not shown).

For one set of results a downward flow velocity of  $150 \text{ m s}^{-1}$  is imposed on the  $\text{H}^+$  ions at 1400 km inside the plasmasphere; for the other, the velocity is zero. The results show that at

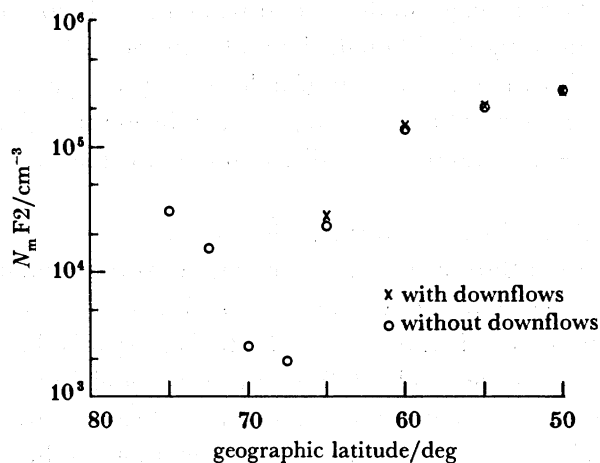


FIGURE 5. Modelled values of peak electron concentration in the F-layer along the meridian through EISCAT for 17h00 U.T.; conditions are appropriate to Northern Hemisphere winter under moderate sunspot activity ( $F_{10.7} = 120$ ). Results  $\circ$  have zero downflow of  $\text{H}^+$  at the upper boundary inside the plasmasphere; results  $\times$  have imposed downflow velocity at upper boundary (see text).

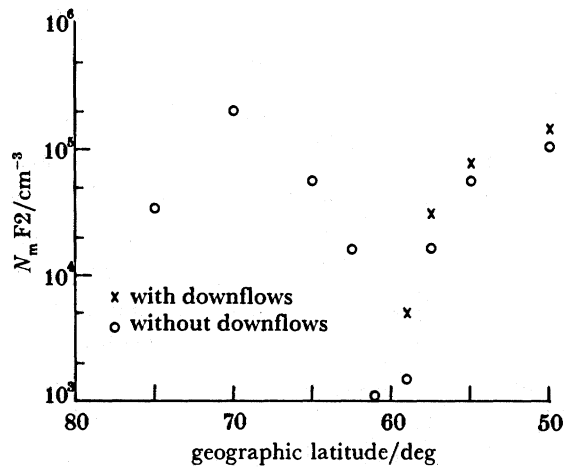


FIGURE 6. As for figure 5 except that time is 23h00 U.T.

17h00 U.T. (figure 5) the downflow signature is barely evident. By 23h00 U.T. (figure 6) the effects of the downflow are significant and obscure the original zero-flow equatorward portion of the trough. Results for 05h00 U.T. (not shown) show that these effects persist until dawn and cannot be ignored for realistic modelling of the mid-latitude trough. The imposed velocity of  $150 \text{ m s}^{-1}$  is based on mid-latitude results of Murphy *et al.* (1976), who demonstrated that  $\text{H}^+$  flows into the topside may perturb F-layer ion concentrations by up to 15%.

### (c) The polar wind

It has been predicted that on the open field lines of the polar cap and on closed field lines with a low  $\text{H}^+$  content the difference in plasma pressure between the ionosphere and the magnetosphere should drive an outflow of the light ions,  $\text{H}^+$  and  $\text{He}^+$ . Raitt & Schunk (1983), Moore (1984) and Yau & Lockwood (1989) have reviewed the theory and experimental observations of the polar wind. Raitt & Schunk state that 'theoretical modelling has far outstripped experimental observations'. The most recent experimental observation appears to be that by Nagai *et al.* (1984). These authors used results from the retarding ion mass spectrometer (RIMS) instrument on board the *Dynamics Explorer 1* spacecraft to verify the supersonic nature of the polar wind at altitude of around  $2R_E$ . The polar wind flux of ions of a few electronvolts in energy was found to be  $2.6 \times 10^8 \text{ cm}^{-2} \text{ s}^{-1}$ . No statistical information on the polar wind outflow is yet available from the RIMS data-set.

The value of the escape flux of  $\text{H}^+$  from the ionosphere to the magnetosphere has recently become a key parameter in the discussion of the source of magnetospheric plasma (T. E. Moore *et al.*, this Symposium; Shelley 1985; Chappell *et al.* 1987). Unfortunately, in this key area, most models produce upper and/or lower bounds for the escape flux of thermal  $\text{H}^+$  and are unable to specify the value that is expected actually to be attained for given geophysical conditions. Raitt & Schunk (1983) conclude that the  $\text{H}^+$  flux should vary from  $10^7$  to  $5 \times 10^8 \text{ cm}^{-2} \text{ s}^{-1}$ , depending on the geophysical conditions, and it is difficult for present-day models to be more precise than this. The models of Gombosi *et al.* (1985), Ganguli *et al.* (1987) and Barakat *et al.* (1987), for example, make several important and interesting predictions about such topics as the effects of ion heating, anisotropic temperatures and the dependence of flux upper bounds on solar activity. Certainly, theoretical modelling in these areas continues

to outstrip experimental observations. But little guidance is obtained on the actual escape flux of  $H^+$  under quiet conditions. For example, Ganguli *et al.* (1987) assume that at 1500 km altitude the  $H^+$  flux is  $1.28 \times 10^8 \text{ cm}^{-2} \text{ s}^{-1}$  and then integrate the  $H^+$  and  $O^+$  equations upwards; of course, the  $H^+$  flux (times the area of tube) is conserved.

Calculations using the high-latitude model of Allen *et al.* (1986) are relevant to the escape flux in the polar wind. As mentioned just above and in §4 the  $H^+$  field-aligned velocity at a specified great altitude has not yet been theoretically derived. Allen *et al.* (1986) elected to raise the upper boundary of a previous model (Quegan *et al.* 1982) to the 10000 km level; the imposed  $H^+$  velocity values were adjusted to give  $H^+$  velocities at 1400 km that agree on average with the Isis-2 observations by Hoffman & Dodson (1980). The results have now been recast to give ion fluxes in the topside ionosphere; results have also been obtained for other geophysical conditions (still, however, using the *msis-77* empirical thermospheric model).

The variability of  $H^+$  fluxes in the high-latitude ionosphere (poleward of  $50^\circ$  latitude) is demonstrated in figure 7. The  $O^+$  and  $He^+$  fluxes (and the  $H^+$  fluxes under different conditions) show similar, but not necessarily corresponding, variability. Of more significance in the present discussion are the average values predicted for the ion fluxes over particular ranges of latitude, where results such as those of figure 7 have been interpolated onto a uniform distribution of grid points. A selection of these average values is presented in tables 1 and 2.

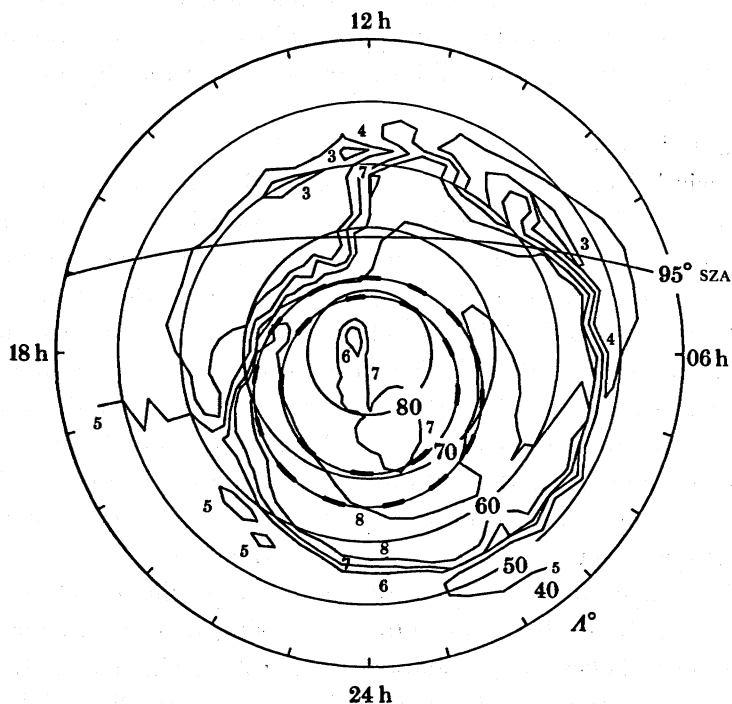


FIGURE 7. Calculated  $H^+$  fluxes in the high-latitude topside ionosphere as a function of latitude and magnetic local time under winter, solar minimum conditions (at 1400 km,  $F_{10.7} = 70$ ). The terminator plotted is the  $95^\circ$  solar zenith angle contour; the region between the large-dashed curves is the location of the assumed auroral ionization zone (Allen *et al.* 1986). Contours (per centimetre squared per second): 8,  $10^8$ ; 7,  $10^7$ ; 6,  $10^6$ ; 5, 0; 3,  $-10^7$ ; 4,  $-10^6$ .

The flux values of table 1 show how insensitive the  $H^+$  results are to the upper boundary conditions on the field-aligned velocities. The standard velocity conditions are those used by Allen *et al.* (1986); for the second set of conditions of table 1, the velocity values for  $H^+$  (and



TABLE 1. CALCULATED AVERAGE  $H^+$  FLUXES AT 1400 km AT WINTER SOLSTICE FOR  $F_{10.7} = 70$ 

$H^+$ velocity values at 10000 km	lowest colatitude/deg	flux/( $10^7 \text{ cm}^{-2} \text{ s}^{-1}$ )
standard	20	3.4
	30	3.9
	40	3.4
$2 \times$ standard	20	3.5
	30	4.0
	40	3.5

$He^+$ ) were doubled. The  $O^+$  results (not shown) are more sensitive. Table 1 also demonstrates that the ranges of latitude over which the averages are carried out have little influence on the average  $H^+$  fluxes. This is generally true for  $H^+$  and  $He^+$  under other conditions but is not true for  $O^+$  (results not shown).

Table 2 illustrates the dependence of  $H^+$  and  $He^+$  fluxes on solar activity and season. The  $He^+$  value for winter, solar maximum is a factor of 30 greater than that for summer, solar minimum. This increase is a reflection of the much greater abundance of neutral helium in the winter helium bulge, particularly at solar maximum. In contrast, the empirical decrease of neutral atomic hydrogen abundance with increasing solar activity is compensated by an increase in calculated F-layer  $O^+$  concentrations due to increasing solar ionizing flux. Thus the greatest value of  $H^+$  flux occurs in summer at solar maximum. Taking latitudes poleward of  $60^\circ$ , giving a surface area of  $1 \times 10^{18} \text{ cm}^2$  (corresponding to table 2 and in accord with Yau & Lockwood (1989)), the calculated polar wind contribution to the magnetospheric plasma lies between  $3.3 \times 10^{25}$  and  $8.5 \times 10^{25} H^+$  ions per second and between  $2.1 \times 10^{23}$  and  $6.4 \times 10^{24} He^+$  ions per second. This contribution, of course, pertains only to the strictly thermal energy part of the polar wind. No attempt has been made to incorporate low-altitude acceleration mechanisms or to simulate high-altitude acceleration processes by imposition of upward fluxes of  $O^+$ ,  $H^+$  and  $He^+$  in the topside ionosphere.

TABLE 2. CALCULATED AVERAGE  $H^+$  AND  $He^+$  FLUXES AT 1400 km FOR LATITUDES POLEWARD OF  $60^\circ$ 

solar activity	season	$H^+$ /( $10^7 \text{ cm}^{-2} \text{ s}^{-1}$ )	$He^+$ /( $10^6 \text{ cm}^{-2} \text{ s}^{-1}$ )
$F_{10.7} = 70$	winter	3.9	1.90
	summer	3.3	0.21
$F_{10.7} = 150$	winter	3.8	6.40
	summer	8.5	0.47

(d) *Effects of  $E \times B$  drifts at mid-latitudes*

As remarked in §2, many useful applications of mid-latitude ionosphere models do not demand an  $E \times B$  drift (apart from the natural corotation with the Earth's motion). There are occasions, however, when the observed data are being used to derive  $E \times B$  drifts or when the drifts are likely to have significant effects on the simulated parameters.

An example of the first class is illustrated in figures 8 and 9. The group delay and Doppler shift of whistler-mode signals that have traversed the magnetosphere (in field-aligned electron density ducts) are often analysed to give the plasma content of the tube of plasma, the time derivative of the content (in units of flux) and the  $E \times B$  drift velocity of the tube of plasma. In particular, antennae at Faraday station in Antarctica detect signals from the North

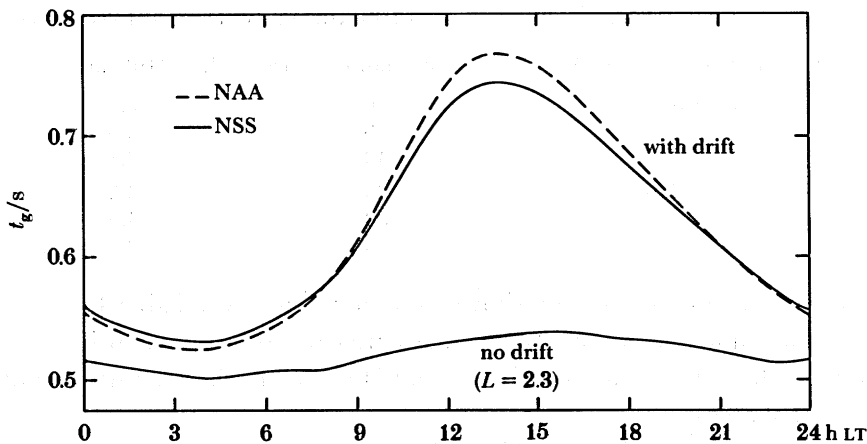


FIGURE 8. Predictions from a model plasmasphere of the group delay on whistler-mode signals transmitted at NAA and NSS radio stations and observed at Faraday via field-aligned plasmaspheric ducts. In the no-drift case (just one curve shown) the  $L$ -value is fixed at 2.3; in the drift cases the imposed equatorial drift velocity and consequent variation in  $L$ -value are those shown in figure 9.

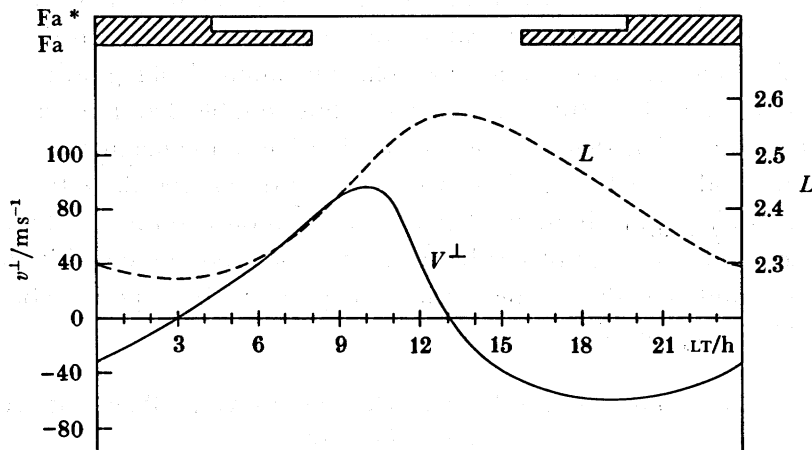


FIGURE 9. The equatorial drift velocity (solid curve), and the consequent  $L$ -value (dashed curve) used to obtain the results (with drift) of figure 8. Nighttime at Faraday (Fa) and at its conjugate in the Northern Hemisphere (Fa\*) is indicated by the hatched areas; conditions used are those for July 1986, with the neutral atmosphere and solar zenith angle appropriate to the Faraday geographic latitude.

American radio stations NAA and NSS (Smith *et al.* 1987). In figure 8 are contrasted the group delays predicted by ionosphere models: in one case zero drift is assumed and in the other a diurnally varying empirical drift is imposed (see figure 9). The increase in group delay as the model tube of plasma moves poleward reflects the increase in the volume of the tube with increasing  $L$ -value. As the tube retreats towards its initial  $L$ -value (after about 13h00 LT) the group delay declines. The NAA and NSS curves cross each other, showing the dependence of group delay on whistler frequency. These features are in accord with observed data; indeed, it is this behaviour (plus that of the Doppler shift) that the experimenters use to deduce the  $\mathbf{E} \times \mathbf{B}$  drift and the rate of change of tube content.

The zero-drift case of group delay in figure 8 shows only a small variation during the 24 h; this variation is due to the effects of the ionosphere-magnetosphere plasma fluxes. It can be observed that when the drifting (and corotating) tube returns to  $L = 2.3$  (at around midnight

and 06h00 LT), the group delay for the drifting tube differs from that of the tube which is stationary in the meridional plane. The expansion and contraction of the tube over the 24-hour period lead to competing effects on the tube content that do not quite cancel. At these latitudes the net effect is small. At higher latitudes, however, as magnetospheric electric fields penetrate and the average tube volume increases, the effects are likely to be significant. Not only is it expected that tube content (and thus the rate of refilling of tubes) will be affected but also that the redistribution of plasma in a drifting tube will lead to marked effects on field-aligned fluxes of  $H^+$  and  $He^+$  in the upper reaches of the tube. Some of the marked  $H^+/He^+$  field-aligned counterstreaming effects observed at great altitudes by Chandler & Chappell (1986) may be as a result of  $E \times B$  drifts.

## 6. CONCLUDING REMARKS

Great strides have been made in recent years in the modelling of the ionosphere and plasmasphere under magnetically quiet conditions. Some of the advances for the F-region and topside ionosphere are illustrated in §5. It is also apparent from §5 that there remain limitations in our knowledge of certain input parameters and on the capacity to model certain processes.

Electric fields generated in the E-region and in the magnetosphere have profound effects on the plasmasphere; much remains to be done to delineate them in sufficient detail to predict accurately how the plasmasphere responds. Particle precipitation patterns that are consistent with the convection patterns are also required.

The composition and winds of the neutral atmosphere (in particular the abundances of neutral atomic hydrogen and neutral helium) give rise to uncertainty. It would be helpful if the behaviour of neutral helium could be grafted onto the UCL thermosphere model and in due course onto the UCL–Sheffield thermosphere–ionosphere model. Improvements have been made in modelling electron and ion temperatures at low and mid-latitudes, although there is still debate about electron heating and cooling rates. At high latitudes, the heat flux to the electron gas from the magnetosphere is a major concern. The role of vibrationally excited nitrogen molecules has not been properly explored.

Finally, the challenge of constructing a complete model of the low-energy polar wind is still here, twenty years after the appearance of the papers by Axford and Banks & Holzer. Related to the problem of the polar wind is the process whereby tubes of plasma are ‘peeled off’ the plasmasphere as the strength of the magnetospheric electric field increases in magnetically stormy times. Successful non-steady state and magnetic storm studies will require the resolution of many of these problems.

## REFERENCES

- Allen, B. T., Bailey, G. J. & Moffett, R. J. 1986 *Annls Geophysicae* A 4, 97–106.  
 Bailey, G. J., Moffett, R. J., Simmons, P. A. & Footitt, R. J. 1986 *Annls Geophysicae* A 4, 113.  
 Bailey, G. J., Simmons, P. A. & Moffett, R. J. 1987 *J. atmos. terr. Phys.* 49, 503.  
 Barakat, A. R., Schunk, R. W., Moore, T. E. & Waite, J. H. Jr 1987 *J. geophys. Res.* 92, 12255.  
 Burgers, J. M. 1969 *Flow equations for composite cases*. New York: Academic Press.  
 Chandler, M. O. & Chappell, C. R. 1986 *J. geophys. Res.* 91, 8847.  
 Chappell, C. R., Moore, T. E. & Waite, J. H. Jr 1987 *J. geophys. Res.* 92, 5896.  
 Collis, P. N. & Häggström, I. 1988 *J. atmos. terr. Phys.* 50, 389.  
 Conrad, J. R. & Schunk, R. W. 1979 *J. geophys. Res.* 84, 811.  
 Fuller-Rowell, T. J., Rees, D., Quegan, S., Moffett, R. J. & Bailey, G. J. 1987 *J. geophys. Res.* 92, 7744 and 7775.

- Ganguli, S. B., Mitchell, H. G. Jr & Palmadesso, P. J. 1987 *Planet. Space Sci.* **35**, 703.  
 Gombosi, T., Cravens, T. E. & Nagy, A. F. 1985 *Geophys. Res. Lett.* **12**, 167.  
 Grad, H. 1949 *Communs pure appl. Math.* **2**, 331.  
 Grad, H. 1958 *Handbook Phys.* vol. XII, 205.  
 Hanson, W. B. & Moffett, R. J. 1966 *J. geophys. Res.* **71**, 5556.  
 Heelis, R. A., Hanson, W. B., Bailey, G. J. & Murphy, J. A. 1989 (Submitted.)  
 Hoffman, J. M. & Dodson, W. M. 1980 *J. geophys. Res.* **85**, 626.  
 Iwagami, N. & Ogawa, T. 1982 *Nature, Lond.* **298**, 454.  
 Kendall, P. C. & Pickering, W. M. 1967 *Planet. Space Sci.* **15**, 825.  
 Moffett, R. J. 1979 *Fundamentals Cosmic Phys.* **4**, 313.  
 Moffett, R. J. 1988 *Planet. Space Sci.* **36**, 65.  
 Moffett, R. J. & Hanson, W. B. 1973 *J. atmos. terr. Phys.* **35**, 207.  
 Moffett, R. J. & Quegan, S. 1983 *J. atmos. terr. Phys.* **45**, 315.  
 Moore, T. E. 1984 *Rev. Geophys. Space Phys.* **22**, 264.  
 Muldrew, D. B. 1983 *Radio Sci.* **18**, 1140.  
 Murphy, J. A., Bailey, G. J. & Moffett, R. J. 1976 *J. atmos. terr. Phys.* **38**, 351.  
 Nagai, T., Waite, J. H. Jr, Green, J. L., Chappell, C. R., Olsen, R. C. & Comfort, R. H. 1984 *Geophys. Res. Lett.* **11**, 669.  
 Ogawa, T. 1982 *Planet. Space Sci.* **30**, 39.  
 Quegan, S., Bailey, G. J. & Moffett, R. J. 1981 *Planet. Space Sci.* **29**, 851.  
 Quegan, S., Bailey, G. J., Moffett, R. J., Heelis, R. A., Fuller-Rowell, T. J., Rees, D. & Spiro, R. W. 1982 *J. atmos. terr. Phys.* **44**, 619.  
 Quegan, S., Bailey, G. J. & Moffett, R. J. 1984 *Planet. Space Sci.* **32**, 791.  
 Raitt, W. J. & Schunk, R. W. 1983 *Energetic ion composition in the Earth's magnetosphere* (ed. R. G. Johnson), pp. 99-141. Tokyo: Terra Publishing Co.  
 St-Maurice, J.-P. & Schunk, R. W. 1977 *Planet. Space Sci.* **25**, 907.  
 Schunk, R. W. 1975 *Planet. Space Sci.* **23**, 437.  
 Schunk, R. W. 1987 *Physica Scr. T* **18**, 256.  
 Schunk, R. W. & Sojka, J. J. 1985 *J. geophys. Res.* **90**, 5285.  
 Schunk, R. W., Sojka, J. J. & Bowline, M. D. 1986 *J. geophys. Res.* **91**, 12041.  
 Shelley, E. G. 1985 *Adv. Space Res.* **5**, 401.  
 Smith, A. J., Yearby, K. H., Bullough, K., Saxton, J. M., Strangeways, H. J. & Thomson, N. R. 1987 *Mem. natn Inst. Polar Res., special Issue*, **48**, 183.  
 Sterling, D. L., Hanson, W. B., Moffett, R. J. & Baxter, R. G. 1969 *Radio Sci.* **4**, 1005.  
 Yau, A. W. & Lockwood, M. 1989 (Submitted.)

### Discussion

S. QUEGAN (*University of Sheffield, U.K.*). Could Professor Moffett comment on the connection between his calculated outflows and the concept of 'limiting flux'; in particular, does he consider the concept of 'limiting flux' to be viable (or meaningful) for the convecting high-latitude ionosphere?

R. J. MOFFETT. The idea of 'limiting proton flux' to the protonosphere was examined by workers such as Hanson & Patterson (1967) and Geisler (1964). They were able to derive simple expressions for the flux under straightforward assumptions such as isothermal and steady-state conditions. These ideas have been developed numerically, a recent example being work by Barakat & Schunk and coworkers. However, the 'limiting flux' gives only an upper bound on what may be observed or predicted to occur. In the paper an attempt was made to refine the actual values that might be expected. For convecting flux tubes under non-steady state conditions it would appear difficult to compute a value for the 'limiting flux' that would be relevant to those conditions; thus the concept is not now a particularly helpful one.

### References

- Geisler, J. E. 1964 *J. geophys. Res.* **72**, 81.  
 Hanson, W. B. & Patterson, T. N. L. 1967 *Planet. Space Sci.* **12**, 979.